Synthesis of vector wave envelopes in three-dimensional random elastic media characterized by a Gaussian autocorrelation function based on the Markov approximation: Plane wave case

Haruo Sato[1]

Received 9 September 2005; revised 7 February 2006; accepted 1 March 2006; published 13 June 2006.

[1] High-frequency seismograms of microearthquakes observed at long travel distances have longer apparent durations than the source durations caused by scattering due to lithospheric inhomogeneity. Frequency dependence of the peak delay from the onset and the broadening of seismogram envelope well reflect the spectra of random velocity inhomogeneity. Here we propose a formulation for the envelope synthesis of vector waves in three-dimensional random elastic media in the case that wavelengths are smaller than the characteristic scale of random inhomogeneity. A stochastic master equation for the two-frequency mutual coherence function (TFMCF) of potential field is derived on the basis of the Markov approximation, which is a stochastic extension of the phase screen method for solving the parabolic wave equation. From the Fourier transform of TFMCF at a given travel distance, we are able to synthesize the mean square traces of three vector wave components. For the incidence of an impulsive plane P wavelet to random elastic media characterized by a Gaussian autocorrelation function, the mean square envelope of each component at a long travel distance is analytically written by using an elliptic theta function. Each synthesized envelope shows peak delay from the onset and broadening with travel distance increasing; however, the peak delay of the transverse component is larger than that of the longitudinal component. For the same fractional velocity fluctuation, the envelope broadening for S waves is larger than that for P waves.

Citation: Sato, H. (2006), Synthesis of vector wave envelopes in three-dimensional random elastic media characterized by a Gaussian autocorrelation function based on the Markov approximation: Plane wave case, *J. Geophys. Res.*, *111*, B06306, doi:10.1029/2005JB004036.

1. Introduction

[2] High-frequency seismograms are complex because of the Earth's inhomogeneity. Especially, coda waves of local earthquakes having smooth envelopes are clear evidence for large-angle scattering caused by small-scale inhomogeneities distributed in the lithosphere. There is another clear evidence of lithospheric inhomogeneity along seismic ray paths that seismogram envelopes are broadened with travel distance increasing. *Douglas et al.* [1973] reported the complexity of direct P wave and P coda of nuclear explosions in 0.5–2.25 Hz band at large epicentral distances of 27°–44°. They discussed a possibility of multipathing due to velocity inhomogeneity. Examining the teleseismic P waves from an explosion recorded at the NORSAR array, *McLaughlin and Anderson* [1987] found a delay of 5-Hz band signals from 1-Hz band signals. Comparing with numerical simulations of P wave propagation through a random medium characterized by a Gaussian autocorrelation function (ACF), they interpreted the observed velocity dispersion to be caused by randomness having multiscale correlation distances. Analyzing teleseismic P waves recorded in the French Massif Central, *Ritter et al.* [1997] reported a delay of 2–4 Hz band signals of about 2–4 s and a longer duration compared with lower-frequency signals. They interpreted the delay of high-frequency signals to be caused by P-to-S scattering due to heterogeneity in the lower crust. Analyzing teleseismic P coda waves, *Nishimura et al.* [2002] found a regional variation of the excitation in the transverse component having a correlation with tectonic settings.

[3] Examining S wave seismogram envelopes of local microearthquakes in Kanto, Japan, *Sato* [1989] found the envelope broadening with travel distance increasing. In eastern North America, *Atkinson* [1993] reported an increase in the duration of S wave trains with increasing travel distance for a distance range from 10 to 500 km. Analyzing array data of local crustal earthquakes in southern California and Nevada, *Wagner* [1997] interpreted that the P and S wave trains are composed predominantly of forward scattered waves with relatively little mode conversions.

[4] *Sato* [1989] interpreted the envelope broadening phenomenon observed in Kanto, Japan by diffraction and forward scattering due to random velocity inhomogeneity

[1]Geophysics, Science, Tohoku University, Sendai, Japan.

0148-0227/06/2005JB004036$09.00

on the basis of the Markov approximation for the parabolic wave equation in the case that wavelengths are shorter than the correlation distance. The Markov approximation is a kind of stochastic extension of the split-step phase screen method, which was extensively developed for the study of optical wave propagation through random media in 1970s [e.g., *Williamson*, 1972; *Shishov*, 1974; *Lee and Jokipii*, 1975a, 1975b; *Sreenivasiah et al.*, 1976]. The validity of the Markov approximation was recently confirmed numerically by a comparison with finite difference simulations for scalar wave propagation through two-dimensional (2-D) random elastic media [*Fehler et al.*, 2000]. Using the envelope inversion with a fixed attenuation factor, *Scherbaum and Sato* [1991] estimated the ratio of the square of fractional fluctuation of velocity inhomogeneity to the correlation distance as $\varepsilon^2/a \approx 0.00054\ \mathrm{km}^{-1}$ from the analysis of envelope broadening of S seismograms of local earthquakes in Kanto, Japan for frequencies from 2 Hz through 16 Hz. Later, *Obara and Sato* [1995] found regional difference of S wave envelopes observed in the Kanto and Tokai area, Japan beneath which the Pacific plate is subducting: envelope broadening is small and independent of frequency on the fore arc side; however, envelope broadening is large especially in high frequencies on the back arc side. They interpreted that the velocity inhomogeneity is rich in short-wavelength spectra beneath the back arc of the volcanic front compared with the fore arc side. Recently, *Saito et al.* [2002] well formulated the envelope broadening of scalar waves radiated from a point source in 3-D random media having a realistic power law spectrum.

[5] *Gusev and Abubakirov* [1996] simulated envelope broadening in nonisotropic scattering media by using the Monte Carlo method. *Gusev and Abubakirov* [1999a] proposed an inversion of envelope broadening for the medium inhomogeneity, and then *Gusev and Abubakirov* [1999b] and *Petukhin and Gusev* [2002] applied it to Kamchatka data and revealed the depth profile of scattering strength. *Korn* [1993, 1997] and *Hock et al.* [2004] applied a heuristic approach based on the energy flux model to the envelope analysis of teleseismic P waves for the study of medium heterogeneity.

[6] All the above approaches are qualitatively successful for explaining the envelope broadening phenomena; however, they are energetic approaches based on the radiative transfer theory or scalar wave models in media having random velocity fluctuation. That is, it is very necessary to develop the envelope synthesis of vector waves. Recently, *Korn and Sato* [2005] proposed an extension of the Markov approximation to vector wave envelopes in 2-D random elastic media. They succeeded in deriving vector wave envelopes of two components for the incidence of an impulsive plane wavelet by using the angular spectrum of potential field. H. Sato and M. Korn (Synthesis of cylindrical vector wave envelopes in 2-D random elastic media based on the Markov approximation, preprint, 2006, hereinafter referred to as Sato and Korn, preprint, 2006) theoretically derived envelopes of cylindrically outgoing vector waves for an impulsive radiation from a point source in 2-D random elastic media in more rigorous manner. They showed a good coincidence of their direct simulation envelopes with envelopes of waves simulated by the finite difference method for the case of P waves.

[7] Here, we propose a direct synthesis of vector wave envelopes in 3-D random elastic media as an extension of the method used for the 2-D case of Sato and Korn (preprint, 2006). When the wavelength is smaller than the characteristic scale of medium inhomogeneity, P and S waves can be treated separately and each potential field is governed by a parabolic wave equation. A stochastic master equation for the two-frequency mutual coherence function of potential field can be derived based on the Markov approximation. Intensity of each vector component can be calculated from the Fourier transform of the two-frequency mutual coherence function. For the case of random elastic media characterized by a Gaussian autocorrelation function, an analytical expression is obtained for each vector component envelope.

2. Markov Approximation

2.1. Wave Equation in Random Media

2.1.1. Parabolic Wave Equation for the Case of Short Wavelengths

[8] Locally isotropic inhomogeneous elastic media are characterized by Lame coefficients λ and μ and mass density ρ, which are functions of coordinate $\mathbf{x}$ in the three-dimensional space. The displacement vector $\mathbf{u}(\mathbf{x}, t)$ is governed by the equation

$$\rho\ddot{u}_i = \left(\lambda u_{l,l}\right)_{,j} + \left(\mu\left(u_{i,j} + u_{j,i}\right)\right)_{,j}. \tag{1}$$

Introducing scalar potential ϕ and vector potential $\mathbf{B}$ as $\mathbf{u} = \nabla\phi + \nabla \times \mathbf{B}$, we may write the above equation as follows:

$$\begin{aligned}\rho\left(\ddot{\phi}_{,i} + \varepsilon_{ilm}\partial_l\ddot{B}_m\right) = {} & \lambda_{,i}\Delta\phi + \mu_{,j}\left(\phi_{,ij} + \varepsilon_{ilm}\partial_l B_{m,j} + \phi_{,ji} + \varepsilon_{jlm}\partial_l B_{m,i}\right) \\ & + (\lambda + 2\mu)\Delta\phi_{,i} + \mu\varepsilon_{ilm}\partial_l\Delta B_m.\end{aligned} \tag{2}$$

When the wavelength is smaller than the characteristic scale (correlation distance) a of medium inhomogeneity, spatial derivatives of elastic parameters can be neglected. In this case, there is no conversion between P and S waves, which can be treated independently. Each potential is independently governed by the following wave equation:

$$\Delta\phi - \frac{1}{\alpha^2}\ddot{\phi} = 0 \quad \text{and} \quad \Delta\mathbf{B} - \frac{1}{\beta^2}\mathbf{B} = 0, \tag{3}$$

where $\alpha = \sqrt{(\lambda + 2\mu)/\rho}$ and $\beta = \sqrt{\mu/\rho}$ are P and S wave velocities, respectively.

[9] We imagine elastic media, which are homogeneous (α and β are constant) in a half-space of $z < 0$ and are inhomogeneous (α and β are nonuniform) in a half-space of $z > 0$. We study wave propagation for $z > 0$ for the incidence of an impulsive plane wavelet from $z < 0$ to the z direction. Figure 1 schematically illustrates wave traces after travelling through a randomly inhomogeneous medium for the incidence of an impulsive P wavelet.

[10] We first study the propagation of P waves, where the P wave velocity has a fractional fluctuation $\xi(\mathbf{x})$ around the average velocity V_0: $\alpha(\mathbf{x}) = V_0(1 + \xi(\mathbf{x}))$. When the

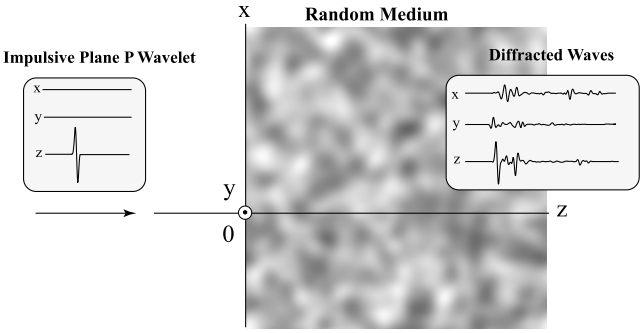

Figure 1. Schematic illustration of vector wave propagation through a random medium spreading over a half-space for the incidence of an impulsive plane P wavelet.

fractional fluctuation is small ($|\xi| \ll 1$), the wave equation for the scalar potential is written as

$$\Delta\phi - \frac{1}{V_0^2}\ddot{\phi} + \frac{2}{V_0^2}\xi(\mathbf{x})\ddot{\phi} = 0. \tag{4}$$

For P waves having a global ray to the z direction, the potential is written as a superposition of plane waves of angular frequency ω as

$$\phi(\mathbf{x}_\perp, z, t) = \frac{1}{2\pi}\int_{-\infty}^{\infty} d\omega e^{ik_0 z - i\omega t}\frac{1}{ik_0}U(\mathbf{x}_\perp, z, \omega), \tag{5}$$

where $k_0 = \omega/V_0$ is wave number and $\mathbf{x}_\perp = (x, y)$ is the transverse coordinate. Since the variation of U for an increment in the z direction is small because the wavelength is smaller that the characteristic distance, $ak_0 \gg 1$, we have the parabolic wave equation for U as

$$2ik_0\partial_z U + \Delta_\perp U - 2k_0^2\xi(\mathbf{x})U = 0, \tag{6}$$

where $\Delta_\perp \equiv \partial_x^2 + \partial_y^2$ is a Laplacian in the transverse plane. The parabolic wave equation well describes small angle scattering around the forward direction. Waves arriving just after the direct wave are composed of such small angle scattering waves.

[11] For S wave propagation, we have the same equation for the vector potential of S waves if we put $\beta(\mathbf{x}) = V_0(1 + \xi(\mathbf{x}))$. We will discuss the case of S waves later.

2.1.2. Ensemble of Random Elastic Media

[12] We imagine an ensemble of random media $\{\xi(\mathbf{x})\}$, where the fractional fluctuation $\xi(\mathbf{x})$ is assumed to be a statistically random function of space coordinate $\mathbf{x}$ and $\langle\xi(\mathbf{x})\rangle = 0$, where angular brackets mean the average over the ensemble. The statistical measure of randomness is quantitatively described by an autocorrelation function (ACF), $R(\mathbf{x}) \equiv \langle\xi(\mathbf{x}')\,\xi(\mathbf{x}' + \mathbf{x})\rangle$, which is characterized by a correlation distance a and a mean square (MS) fractional fluctuation $\varepsilon^2 \equiv \langle R(\mathbf{x} = 0)\rangle$. The randomness is supposed to be statistically homogeneous and isotropic, which means that ACF is a function of lag distance $|\mathbf{x}|$ only.

2.1.3. Stochastic Master Equation for the Two-Frequency Mutual Coherence Function

[13] We define the two-frequency mutual coherence function (TFMCF) as a correlation of U between different two locations on the transverse plane (x-y plane) and different angular frequencies at ω' and ω'' at a distance z [e.g., *Ishimaru*, 1978],

$$\Gamma_2(\mathbf{x}'_\perp, \mathbf{x}''_\perp, z, \omega', \omega'') \equiv \langle U(\mathbf{x}'_\perp, z, \omega')U(\mathbf{x}''_\perp, z, \omega'')^*\rangle. \tag{7}$$

This is a key function since the wavefield intensity can be derived from its Fourier transform with respect to the difference angular frequency. Multiplying U by (6) and taking the ensemble average, we obtain the master equation for the TFMCF as

$$2i\partial_z\Gamma_2 + \left(\frac{\Delta'_\perp}{k'_0} - \frac{\Delta''_\perp}{k''_0}\right)\Gamma_2 - 2\langle(k'_0\xi' - k''_0\xi'')U'U''^*\rangle = 0, \tag{8}$$

where U' and U'' mean that their arguments are $(\mathbf{x}'_\perp, \omega')$ and $(\mathbf{x}''_\perp, \omega'')$, respectively. To evaluate the last term, we follow the simple derivation according to *Lee and Jokipii* [1975a]. From (6), we can write the wavefield at z in an integral form by using the wavefield at $z - \Delta z$:

$$U(\mathbf{x}_\perp, z, \omega) \approx U(\mathbf{x}_\perp, z - \Delta z, \omega) + \frac{i}{2k_0}\Delta z\Delta_\perp U(\mathbf{x}_\perp, z - \Delta z, \omega) - ikU(\mathbf{x}_\perp, z - \Delta z, \omega)\int_{z-\Delta z}^{z} dz'\,\xi(\mathbf{x}_\perp, z'), \tag{9}$$

where we suppose the existence of an intermediate scale Δz, which is larger than the correlation distance a but smaller than the scale of variation of U. Substituting (9) into the last term of (8), and taking the ensemble average, we have

$$\langle(k'_0\xi' - k''_0\xi'')U'U''^*\rangle = -\frac{i}{2}\left[(k'^2_0 + k''^2_0)A(0) - 2k'_0k''_0A(|\mathbf{x}'_\perp - \mathbf{x}''_\perp|)\right]\Gamma_2, \tag{10}$$

where backward scattering is neglected and the causality is used. The longitudinal integral of the ACF along the z axis is defined by

$$A(r_\perp) \equiv \int_{-\infty}^{\infty} dz\,R(\mathbf{x}_\perp, z), \tag{11}$$

where $r_\perp \equiv \sqrt{x^2 + y^2}$ is the transverse distance. Substituting (10) into (8), we get the master equation for TFMCF, which is called the Markov approximation. For waves having a global ray to the z direction, TFMCF is independent of center of mass transverse coordinate $\mathbf{x}_{\perp c} = (\mathbf{x}'_\perp + \mathbf{x}''_\perp)/2$ and becomes a function of difference transverse coordinate $\mathbf{x}_{\perp d} = \mathbf{x}'_\perp - \mathbf{x}''_\perp$ because of the homogeneity of randomness. Furthermore, TFMCF is a function of $r_{\perp d} \equiv |\mathbf{x}_{\perp d}|$ because of the isotropy of randomness.

[14] For the case of quasi-monochromatic waves ($\omega_d \ll \omega_c$) propagating a long distance, the dominant contribution of incoherent diffracted waves is strongly controlled by the longitudinal integral of ACF A at a short offset in the transverse plane, $r_{\perp d} \ll a$ [see *Lee and Jokipii*, 1975a; *Ishimaru*, 1978; *Sato and Fehler*, 1998]. Then the stochastic master equation is given by

$$\partial_z\Gamma_2 + i\frac{k_d}{2k_c^2}\Delta_{\perp d}\Gamma_2 + k_c^2[A(0) - A(r_{\perp d})]\Gamma_2 + \frac{k_d^2}{2}A(0)\Gamma_2 = 0, \tag{12}$$

where $k_c = (k_0' + k_0'')/2$ and $k_d = k_0' - k_0''$. We can solve the master equation for Γ_2 using the factorization

$$\Gamma_2 = {}_0\Gamma_2\, e^{-A(0)k_d^2 z/2}. \tag{13}$$

The master equation for ${}_0\Gamma_2$ is given by

$$\partial_z\, {}_0\Gamma_2 + i\frac{k_d}{2k_c^2}\Delta_{\perp d}\, {}_0\Gamma_2 + k_c^2[A(0) - A(r_{\perp d})]\, {}_0\Gamma_2 = 0. \tag{14}$$

Alternative derivations based on a functional formulation are given by *Tatarskii* [1971] and/or *Ishimaru* [1978]. The range of application conditions for this approximation is discussed in detail by *Barabanenkov et al.* [1971].

2.2. P Wave Envelopes

2.2.1. Intensities

[15] Intensity of each component is given by an ensemble average of the square of displacement vector component. For the case of P waves, the x component intensity is given by

$$\begin{aligned} I_x^P(\mathbf{x}_\perp, z, t) &\equiv \left\langle |u_x(\mathbf{x}_\perp, z,\ t)|^2 \right\rangle \\ &= \left\langle \partial_{x'}\phi(\mathbf{x}_\perp', z,\ t)\ \partial_{x''}\phi(\mathbf{x}_\perp'', z,\ t)^* \right\rangle_{\mathbf{x}'=\mathbf{x}''} \\ &= \frac{1}{2\pi}\int_{-\infty}^{\infty} d\omega' e^{ik_0' z - i\omega' t}\frac{1}{2\pi} \\ &\quad \cdot \int_{-\infty}^{\infty} d\omega'' e^{-ik_0'' z + i\omega'' t}\frac{1}{k_0' k_0''}\left\langle \partial_{x'} U' \partial_{x''} U''^* \right\rangle_{\mathbf{x}'=\mathbf{x}''} \\ &= \frac{1}{2\pi}\int_{-\infty}^{\infty} d\omega_c\, \widehat{I}_x^P(z, t, \omega_c). \end{aligned} \tag{15}$$

In the last line, the integrant gives the definition of the intensity spectral density $\widehat{I}_x^P(z,\ t,\ \omega_c)$, which represents the MS envelope of band-pass-filtered trace at central angular frequency ω_c. Putting $\partial_{x'} = \partial_{x_d}$ and $\partial_{x''} = -\partial_{x_d}$ since Γ_2 is independent of the center of mass coordinate and using $1/(k_0' k_0'') \approx 1/k_c^2$, we may write the intensity spectral density as

$$\begin{aligned} \widehat{I}_x^P(z, t, \omega_c) = \frac{1}{2\pi}\int_{-\infty}^{\infty} d\omega_d e^{-i\omega_d(t - z/V_0)} \\ \cdot \left[-\frac{1}{k_c^2}\partial_{x_d}^2 \Gamma_2(\mathbf{x}_{\perp d}, z, \omega_c, \omega_d)\right]_{\mathbf{x}_{\perp d}=0}. \end{aligned} \tag{16}$$

We note that the intensity spectral density is independent of transverse location $\mathbf{x}_\perp$ because of the homogeneity of randomness. Taking the same procedure, we have the y component intensity as

$$\begin{aligned} I_y^P(\mathbf{x}_\perp, z, t) &\equiv \left\langle |u_y(\mathbf{x}_\perp, z,\ t)|^2 \right\rangle \\ &= \left\langle \partial_{y'}\phi(\mathbf{x}_\perp', z,\ t)\ \partial_{y''}\phi(\mathbf{x}_\perp'', z,\ t)^* \right\rangle_{\mathbf{x}'=\mathbf{x}''} \\ &= \frac{1}{2\pi}\int_{-\infty}^{\infty} d\omega' e^{ik_0' z - i\omega' t}\frac{1}{2\pi} \\ &\quad \cdot \int_{-\infty}^{\infty} d\omega'' e^{-ik_0'' z + i\omega'' t}\frac{1}{k_0' k_0''}\left\langle \partial_{y'} U' \partial_{y''} U''^* \right\rangle_{\mathbf{x}'=\mathbf{x}''} \\ &= \frac{1}{2\pi}\int_{-\infty}^{\infty} d\omega_c\, \widehat{I}_y^P(z, t, \omega_c)\ , \end{aligned} \tag{17}$$

where the last line gives the definition of the intensity spectral density as

$$\begin{aligned} \widehat{I}_y^P(z, t, \omega_c) = \frac{1}{2\pi}\int_{-\infty}^{\infty} d\omega_d e^{-i\omega_d(t - z/V_0)} \\ \cdot \left[-\frac{1}{k_c^2}\partial_{y_d}^2 \Gamma_2(\mathbf{x}_{\perp d}, z, \omega_c, \omega_d)\right]_{\mathbf{x}_{\perp d}=0}. \end{aligned} \tag{18}$$

Because of the isotropy of randomness, we have

$$\widehat{I}_x^P(z, t, \omega_c) = \widehat{I}_y^P(z, t, \omega_c). \tag{19}$$

The z component intensity is given by

$$\begin{aligned} I_z^P(\mathbf{x}_\perp, z, t) &\equiv \left\langle |u_x(\mathbf{x}_\perp, z,\ t)|^2 \right\rangle \\ &= \left\langle \partial_z\phi(\mathbf{x}_\perp', z,\ t)\, \partial_z\phi(\mathbf{x}_\perp'', z,\ t)^* \right\rangle_{\mathbf{x}'=\mathbf{x}''} \\ &= \frac{1}{2\pi}\int_{-\infty}^{\infty} d\omega' e^{ik_0' z - i\omega' t}\frac{1}{2\pi}\int_{-\infty}^{\infty} d\omega'' e^{-ik_0'' z + i\omega'' t} \\ &\quad \cdot \left\langle \left(U' + \frac{\partial_z U'}{ik_0'}\right)\left(U''^* - \frac{\partial_z U''^*}{ik_0''}\right)\right\rangle_{\mathbf{x}'=\mathbf{x}''} \\ &= \frac{1}{2\pi}\int_{-\infty}^{\infty} d\omega_c\, \widehat{I}_z^P(z, t, \omega_c)\ , \end{aligned} \tag{20}$$

where the last line gives the definition of the intensity spectral density. Substituting the leading term of (6) $\partial_z U \approx (i/2k_0)\Delta_\perp U$ into (20) and neglecting the product $\Delta_\perp' U' \Delta_\perp'' U''^*$, we may approximate the z component intensity spectral density as

$$\begin{aligned} \widehat{I}_z^P(z, t, \omega_c) = \frac{1}{2\pi}\int_{-\infty}^{\infty} d\omega_d e^{-i\omega_d(t - z/V_0)} \\ \cdot \left[\left(1 + \frac{\Delta_{\perp d}}{k_c^2}\right)\Gamma_2(\mathbf{x}_{\perp d}, z, \omega_c, \omega_d)\right]_{\mathbf{x}_{\perp d}=0}, \end{aligned} \tag{21}$$

where $\Delta_\perp' = \Delta_\perp'' = \Delta_{\perp d}^2$ and $1/k_0'^2 + 1/k_0''^2 \approx 2/k_c^2$ are used.

[16] Here we define the reference intensity spectral density as

$$\widehat{I}^R(z, t, \omega_c) \equiv \frac{1}{2\pi}\int_{-\infty}^{\infty} d\omega_d e^{-i\omega_d(t - z/V_0)}\Gamma_2(\mathbf{x}_{\perp d} = 0, z, \omega_c, \omega_d). \tag{22}$$

By using (22) with (19), we may write (21) as

$$\begin{aligned} \widehat{I}_z^P(z, t, \omega_c) &= \widehat{I}^R(z, t, \omega_c) - \widehat{I}_x^P(z, t, \omega_c) - \widehat{I}_y^P(z, t, \omega_c) \\ &= \widehat{I}^R(z, t, \omega_c) - 2\,\widehat{I}_x^P(z, t, \omega_c)\ . \end{aligned} \tag{23}$$

[17] An impulsive plane P wavelet with unit intensity is written by

$$\widehat{I}_x^P(z, t, \omega_c) = \widehat{I}_y^P(z, t, \omega_c) = 0 \quad \text{and } \widehat{I}_z^P(z, t, \omega_c) = \delta(t - z/V_0) \quad \text{for } z < 0. \tag{24}$$

It is written as the initial condition for the TFMCF:

$$\Gamma_2(\mathbf{x}_{\perp d}, z=0, \omega_c, \omega_d) = {}_0\Gamma_2(\mathbf{x}_{\perp d}, z=0, \omega_c, \omega_d) = 1. \quad (25)$$

2.2.2. Wandering Effect

[18] The Fourier transform of factor $e^{-A(0)k_d^2 z/2}$ in (13) with respect to difference angular frequency gives the wandering effect,

$$w\left(z,\, t-\frac{z}{V_0}\right) \equiv \frac{1}{2\pi}\int_{-\infty}^{\infty} d\omega_d\, e^{-A(0)k_d^2 z/2}\; e^{-i\omega_d(t-z/V_0)} = \frac{V_0}{\sqrt{2\pi A(0) z}} e^{-\frac{V_0^2}{2A(0)z}\left(t-\frac{z}{V_0}\right)^2}, \quad (26)$$

where $\int_{-\infty}^{\infty} dt\, w(z, t-z/V_0) = 1$ and $w(z, t-z/V_0) \to \delta(t)$ as $z \to 0$. It does not mean the broadening of individual wave packets but it shows the wandering effect from the statistical averaging of the traveltime fluctuations of different rays at a distance z [*Lee and Jokipii*, 1975b].

[19] Referring to (22), we define the Fourier transform of ${}_0\Gamma_2$ as the reference intensity spectral density without wandering effect:

$$\widehat{I}_0^R(z,t,\omega_c) = \frac{1}{2\pi}\int_{-\infty}^{\infty} d\omega_d e_0^{-i\omega_d(t-z/V_0)}\, {}_0\Gamma_2(\mathbf{x}_{\perp d}=0, z, \omega_c, \omega_d). \quad (27)$$

The convolution of $\widehat{I}_0^R$ and wandering term w gives the reference intensity spectral density for the incidence of a unit impulsive plane P wavelet, $\widehat{I}^R = \widehat{I}_0^R * w$. In the following, we put subscript "zero" to represent the intensity spectral density without wandering effect: $\widehat{I}_{x0}^P$, $\widehat{I}_{y0}^P$ and $\widehat{I}_{z0}^P$. Convolution with the wandering term w gives the intensity spectral density: $\widehat{I}_x^P = \widehat{I}_{x0}^P * w$, $\widehat{I}_y^P = \widehat{I}_{y0}^P * w$, and $\widehat{I}_z^P = \widehat{I}_{z0}^P * w$. For the practical comparison with ensemble averaged intensity by numerical simulations, we note that it is necessary to convolve the intensity spectral density with the source time function envelope for a given angular frequency $i(t, \omega_c)$: $\widehat{I}_x^P * i$, $\widehat{I}_y^P * i$ and $\widehat{I}_z^P * i$.

2.2.3. Gaussian Autocorrelation Function

[20] In the following, we study the case that random media are characterized by a Gaussian ACF:

$$R(\mathbf{x}) = \varepsilon^2 e^{-r^2/a^2}, \quad (28)$$

where $r \equiv |\mathbf{x}|$. The longitudinal integral for small transverse distances is written as

$$A(r_{\perp d}) \approx \sqrt{\pi}\varepsilon^2 a\left(1 - r_{\perp d}^2/a^2\right) \quad \text{for } r_{\perp d} \ll a. \quad (29)$$

Then, the master equation (14) is explicitly written as

$$\partial_z\, {}_0\Gamma_2 + i\frac{k_d}{2k_c^2}\Delta_{\perp d}\, {}_0\Gamma_2 + \frac{k_c^2\sqrt{\pi}\varepsilon^2 r_{\perp d}^2}{a}\, {}_0\Gamma_2 = 0. \quad (30)$$

This differential equation was solved by *Sreenivasiah et al.* [1976] as

$${}_0\Gamma_2(z, \mathbf{x}_{\perp d}, \omega_c, \omega_d) = \frac{1}{\cos s_0} \mathrm{e}^{-\frac{\tan s_0}{s_0}\frac{2V_0 k_c^2 t_M}{z}\left(x_d^2+y_d^2\right)}, \quad (31)$$

where we define the characteristic time as

$$t_M = \frac{\sqrt{\pi}\varepsilon^2 z^2}{2V_0 a} \quad (32)$$

and a parameter

$$s_0 = 2e^{\frac{\pi}{4}}\sqrt{t_M\omega_d}. \quad (33)$$

2.2.4. Intensity Spectral Density

[21] Taking the Fourier transform of TFMCF, we have the reference intensity spectral density without wandering effect as

$$\begin{aligned}\widehat{I}_0^R(z,t,\omega_c) &= \frac{1}{2\pi}\int_{-\infty}^{\infty} d\omega_d\, e^{-i\omega_d\left(t-\frac{z}{V_0}\right)}\frac{1}{\cos s_0} \\ &= \frac{1}{2\pi}\int_{-\infty}^{\infty} d\omega_d\, e^{-i\omega_d\left(t-\frac{z}{V_0}\right)} \cdot\left[\pi\sum_{k=0}^{\infty}\frac{(-1)^k(2k+1)}{\pi^2\left(k+\frac{1}{2}\right)^2 - 4it_M\omega_d}\right] \\ &= \frac{\pi}{4t_M}\sum_{k=0}^{\infty}(-1)^k(2k+1)\, e^{-\frac{\pi^2}{4t_M}\left(k+\frac{1}{2}\right)^2\left(t-\frac{z}{V_0}\right)} \cdot H\left(t-\frac{z}{V_0}\right) \\ &= \frac{1}{t_M}\frac{\pi}{8}\vartheta_1'\left(0, e^{-\frac{\pi^2(t-z/V_0)}{4\ t_M}}\right)H\left(t-\frac{z}{V_0}\right), \end{aligned} \quad (34)$$

where we used the series expansion

$$\sec s_0 = \pi\sum_{k=0}^{\infty}\frac{(-1)^k(2k+1)}{\pi^2\left(k+\frac{1}{2}\right)^2 - s_0^2}, \quad (35)$$

and the Cauchy integral in the complex ω_d plane. The step function H appears in (34) since all the poles appear only in the lower ω_d plane. In the last line in (34), function

$$\vartheta_1'(v,q) \equiv \frac{\partial}{\partial v}\vartheta_1(v,q)$$

is the derivative of the elliptic theta function ϑ_1 with respect to v, where [e.g., *Wolfram*, 1999, p. 778]

$$\vartheta_1(v,q) \equiv 2\sum_{n=0}^{\infty}(-1)^n q^{(n+1/2)^2}\sin[(2n+1)v]. \quad (36)$$

A solid curve in Figure 2 shows the plot of $\widehat{I}_0^R$ against normalized reduced time $(t-z/V_0)/t_M$. It shows a broadened envelope having a maximum peak of $0.46/t_M$ at $(t-z/V_0)/t_M \approx 0.67$. The peak delay from the onset and the envelope width are scaled by the characteristic time. In the case of Gaussian ACF, the characteristic time is independent of central frequency and it increases with the square of travel distance in proportion to the ratio of MS fractional fluctuation to the correlation distance.

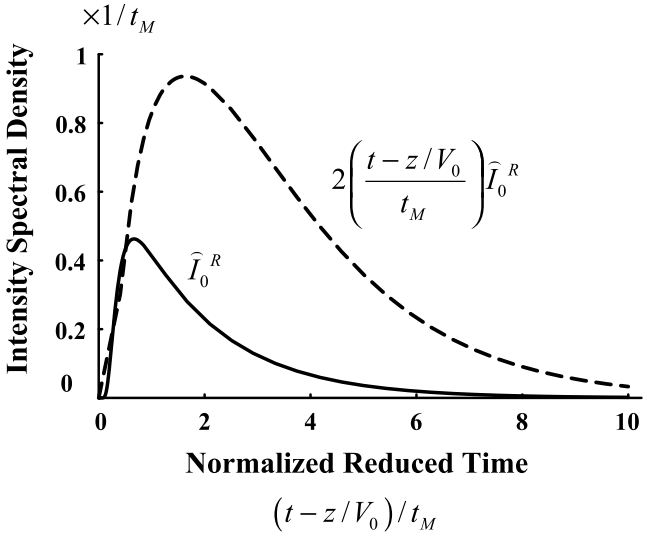

Figure 2. Plots of reference intensity spectral density without wandering effect $\widehat{I}_0^R$ (solid curve) and $2((t - z/V_0)/t_M)\widehat{I}_0^R$ (dashed curve) against normalized reduced time for the incidence of an impulsive plane wavelet.

[22] *Williamson* [1972] derived the same representation as (34) for scalar waves based on the stochastic ray path method. Instead of TFMCF, he derived the master equation for the mutual coherence function for the development of angular spectra. His method treats the successive ray bending process in random media as a stochastic process; however, the calculation of traveltime for each ray path is necessary to synthesize wave envelopes.

[23] Replacing Γ_2 with ${}_0\Gamma_2$ in (16) and (18) and substituting (31) into them, we have the x and y component intensity spectral densities without wandering effect as

$$\begin{aligned}\widehat{I}^P_{x0}(z,t,\omega_c) = \widehat{I}^P_{y0}(z,t,\omega_c) &= \frac{1}{2\pi}\int_{-\infty}^{\infty} d\omega_d e^{-i\omega_d(t-z/V_0)} \\ &\cdot\left[-\frac{1}{k_c^2}\partial^2_{x_d}\,{}_0\Gamma_2(\mathbf{x}_{\perp d}, z, \omega_c, \omega_d)\right]_{\mathbf{x}_{\perp d}=0} \\ &= \frac{4V_0t_M}{z}\frac{1}{2\pi}\int_{-\infty}^{\infty} d\omega_d\, e^{-i\omega_d\left(t-\frac{z}{V_0}\right)}\frac{\tan s_0}{s_0\cos s_0} \\ &= \frac{4V_0t_M}{z}\frac{1}{2\pi}\int_{-\infty}^{\infty} d\omega_d\, e^{-i\omega_d\left(t-\frac{z}{V_0}\right)}\frac{1}{i2\,t_M}\frac{\partial}{\partial\omega_d}\left(\frac{1}{\cos s_0}\right) \\ &= \frac{V_0t_M}{z}\cdot 2\frac{\left(t-\frac{z}{V_0}\right)}{t_M}\cdot\frac{\pi}{8t_M}\vartheta_1'\left(0, e^{-\frac{\pi^2\left(t-z/V_0\right)}{4\ t_M}}\right) \\ &\cdot H\left(t-\frac{z}{V_0}\right) \\ &= \frac{V_0t_M}{z}2\frac{\left(t-\frac{z}{V_0}\right)}{t_M}\widehat{I}^R_0(z,t,\omega_c), \end{aligned} \tag{37}$$

where the explicit representation of the Fourier transform of $1/\cos s_0$ is used. A dashed curve in Figure 2 shows the plot of $2((t - z/V_0)/t_M)\widehat{I}^R_0$ against normalized reduced time. We find $2((t - z/V_0)/t_M)I_0^R$ has its maximum peak of $0.94/t_M$ at normalized reduced time $(t - z/V_0)/t_M \approx 1.63$, which is more than twice that of $\widehat{I}^R_0$.

[24] Putting (37) into (23), we have an explicit representation of the intensity spectral density without wandering effect of z component as

$$\begin{aligned}\widehat{I}^P_{z0}(z,t,\omega_c) &= \left[1-\frac{V_0t_M}{z}\frac{4(t-z/V_0)}{t_M}\right]\widehat{I}^R_0(z,t,\omega_c) \\ &= \left[1-\frac{V_0t_M}{z}\frac{4(t-z/V_0)}{t_M}\right] \\ &\cdot\frac{\pi}{8t_M}\vartheta_1'\left(0, e^{-\frac{\pi^2\left(t-z/V_0\right)}{4\ t_M}}\right)H\left(t-\frac{z}{V_0}\right). \end{aligned} \tag{38}$$

Figure 3 shows plots of $\widehat{I}^P_{x0}$ and $\widehat{I}^P_{y0}$ (dashed line), $\widehat{I}^P_{z0}$ (solid line) and $\widehat{I}^R_0$ (chained line) against normalized reduced time for the case of $V_0t_M/z = 0.05$. As lapse time increases, the intensity spectral densities of x and y components without wandering effect exceed that of the z component, where large incident angle rays dominate over small incident angle rays: $\widehat{I}^P_{0x} > \widehat{I}^P_{0z}$ for $(t - z/V_0)/t_M > z/(6V_0t_M)$. This phenomenon is seen in wave traces in 2-D random elastic media by numerical simulations [see *Korn and Sato*, 2005]. The intensity spectral density without wandering effect of z component become negative for reduced time $(t - z/V_0)/t_M > z/(4V_0t_M)$. It means the breakdown of this approximation for lapse time $t > (5/4)(z/V_0)$.

[25] We note that the wandering term (26) with (29) becomes Gaussian as

$$w\left(z,\, t-\frac{z}{V_0}\right) = \frac{V_0}{\sqrt{2\pi}\sqrt{\pi\varepsilon^2 az}}e^{-\frac{V_0^2}{2\sqrt{\pi\varepsilon^2 az}}\left(t-\frac{z}{V_0}\right)^2}. \tag{39}$$

The time width of wandering effect is proportion to the square root of travel distance.

2.2.5. Characteristics of P Wave Envelopes

[26] Analyzing the correlation between log amplitude and phase fluctuation of teleseismic P waves arriving with near vertical incidence at LASA in Montana, *Aki* [1973] estimated the lithospheric inhomogeneity as $\varepsilon^2/a \approx 0.00016$ km^{-1}. *Flatté and Wu* [1988] estimated a smaller fluctuation from the array analysis of NORSAR data by supposing a power law

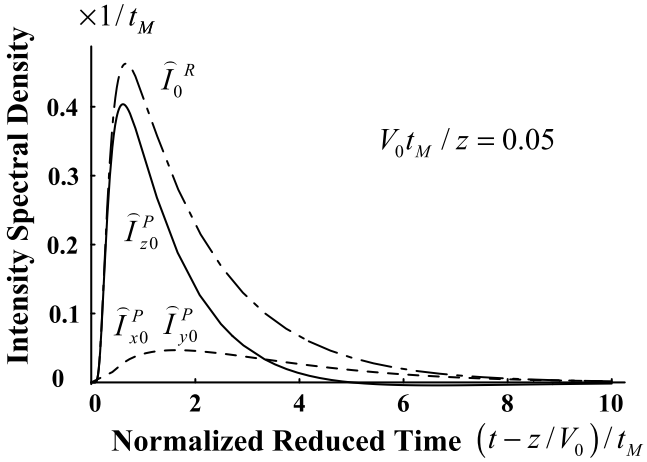

Figure 3. Plots of $\widehat{I}^P_{x0}$, $\widehat{I}^P_{y0}$ and $\widehat{I}^P_{z0}$ with $\widehat{I}^R_0$ against normalized reduced time for the incidence of an impulsive plane P wavelet in the case of $V_0t_M/z = 0.05$.

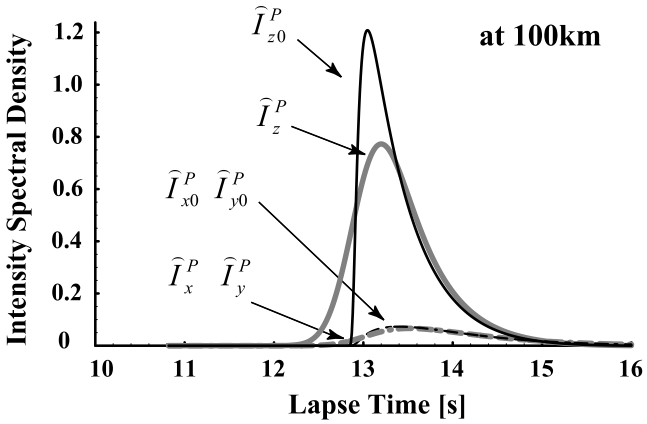

Figure 4. Time traces of intensity spectral densities without wandering effect (black curves) and those with wandering effect (gray curves) at a travel distance of 100 km in random media for the incidence of an impulsive plane P wavelet.

spectra. The ratio $\varepsilon^2/a \approx 0.00054$ km^{-1} obtained from the envelope analysis in Kanto, Japan by *Scherbaum and Sato* [1991] is a few times larger than the estimate of *Aki* [1973]. The difference might be due to the tectonic activities: the former is for island arc and the latter is for stable continent. We take following values typically representing the inhomogeneous lithosphere in the simulation: the background velocities $V_P = 7.8$ km/s and $V_S = 4.5$ km/s($V_P/V_S = 1.73$) and the random inhomogeneity characterized by $\varepsilon = 0.05$ and $a = 8$ km, that is, the ratio $\varepsilon^2/a \approx 0.00031$ km^{-1}. We note that the value $V_0 t_M/z = 0.05$ used in Figure 3 corresponds to the travel distance $z = 182$ km for the choice of these parameter values.

[27] As an example, Figure 4 shows intensity spectral density without wandering effect (black curves) and intensity spectral density with wandering effect (gray curves) at 100km distance for the incidence of an impulsive plane P wavelet to the z direction. We note that the x and y component intensity spectral densities are the same each other. Scattering produces envelope broadening of a large peak in the z component and small peaks in the x and y components; however, the wandering effect causes a collapse of a sharp peak of $\hat{I}^P_{z0}$, but causes little change in dull peaks of $\hat{I}^P_{x0}$ and $\hat{I}^P_{y0}$. The maximum peaks of the x and y components arrive later than the maximum peak of the z component.

[28] Figure 5 (top) shows time traces of intensity spectral densities at four travel distances for the incidence of an impulsive plane P wavelet. Envelope broadening becomes stronger as travel distance increasing. The wandering effect is stronger at longer travel distances; however, apparent contribution to the envelope is stronger at shorter distances since intensity spectral densities without wandering effect has sharper peaks at shorter distances. Figure 6 (top) enlarges time traces of intensity spectral densities in x and

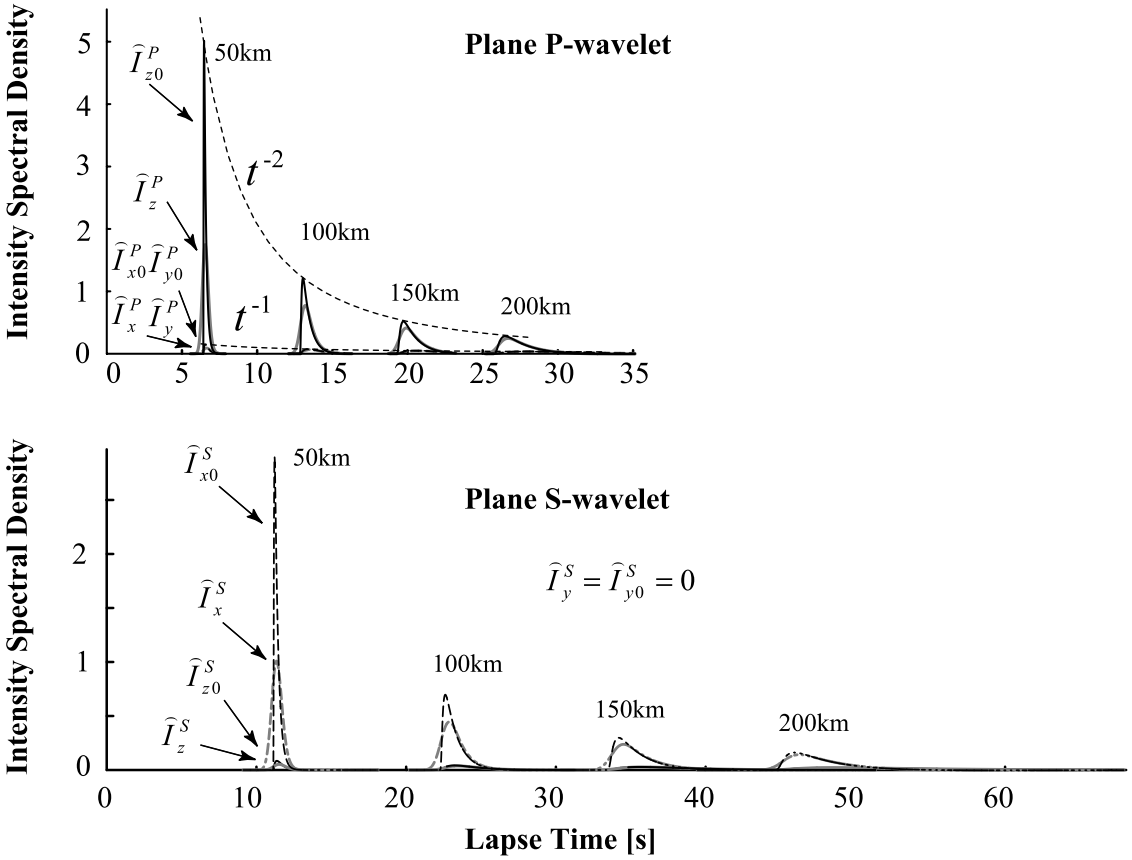

Figure 5. (top) Time traces of intensity spectral densities in random media for the incidence of an impulsive plane P wavelet. (bottom) Those for the incidence of an impulsive plane S wavelet polarized to the x direction.

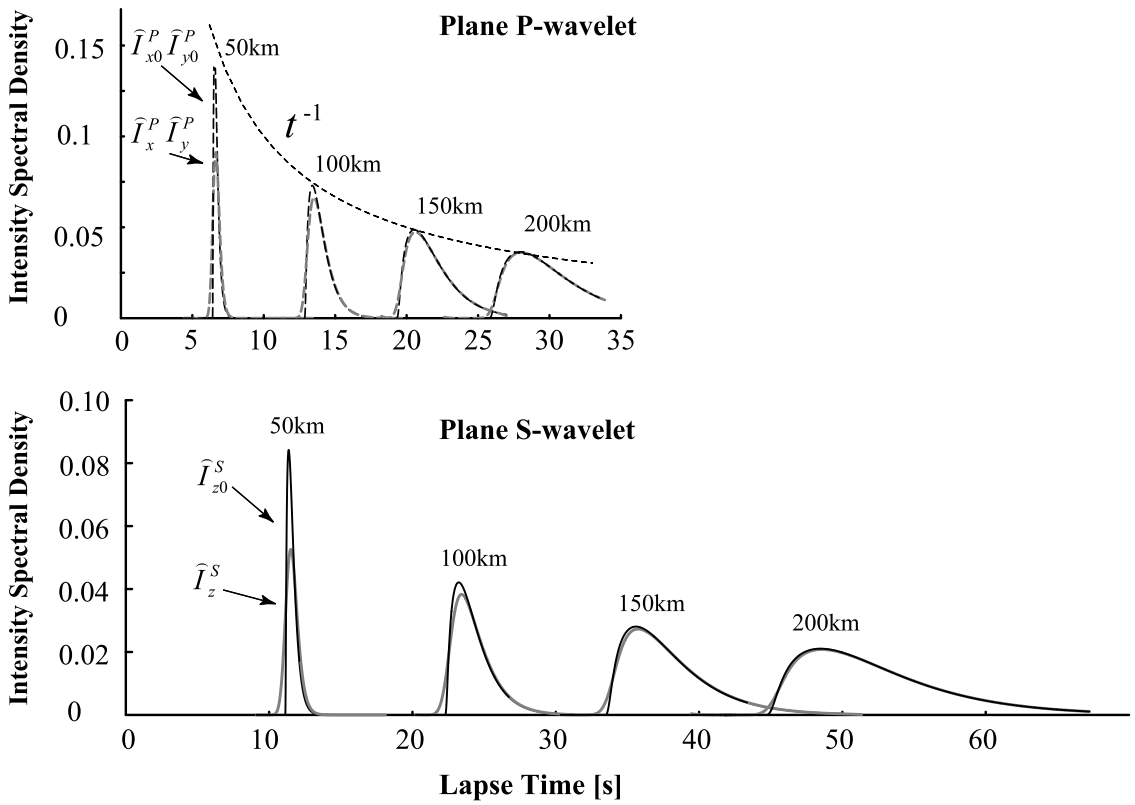

Figure 6. (top) Enlarged view of intensity spectral densities of x component in random media for the incidence of an impulsive plane P wavelet. (bottom) Those of z component for the incidence of an impulsive plane S wavelet polarized to the x direction.

y components. The wandering effect makes little change in envelopes of the x and y components. We should use the intensity spectral density without wandering effect for the analysis of individual wave envelopes; however, it is necessary to use the intensity spectral density with the wandering effect for a comparison with ensemble averaged envelopes of waves numerically simulated as shown by *Fehler et al.* [2000] and *Korn and Sato* [2005].

[29] The time integral of the transverse component intensity spectral density without wandering effect is

$$\int_{z/V_0}^{\infty} \widehat{I}^P_{0x}(z,t,\omega_c)dt = \int_{z/V_0}^{\infty} \widehat{I}^P_{0y}(z,t,\omega_c)dt = \frac{4V_0 t_M}{z} = \frac{2\sqrt{\pi}\varepsilon^2}{a} z \tag{40}$$

since $\lim_{\omega_d \to 0} \tan s_0/(s_0 \cos s_0) = 1$. The integral of intensity spectral density with wandering effect has the same value as (40). That is, the time integral of MS envelope of the transverse component displacement linearly increases with travel distance increasing. We note that

$$\int_{z/V}^{\infty} \widehat{I}^R_0(z,t,\omega_c)dt = 1$$

since $\lim_{\omega_d \to 0} 1/\cos s_0 = 1$. It predicts that the peak values of $\widehat{I}^P_{x0}$ and $\widehat{I}^P_{y0}$ decay approximately according to the inverse of lapse time as shown by a thin dashed curve in Figure 6 (top).

[30] The time integral of the longitudinal component is

$$\int_{z/V_0}^{\infty} \widehat{I}^P_{0z}(z,t,\omega_c)dt = 1 - \frac{8V_0 t_M}{z} = 1 - \frac{4\sqrt{\pi}\varepsilon^2}{a} z. \tag{41}$$

Since the second term is small, we may roughly say that the peak intensity of the z component decreases with the inverse square of travel distance as plotted by thin dashed curve in Figure 5 (top). As discussed below (38), this approximation is valid only for $(t - z/V_0)/t_M < z/(4V_0 t_M)$, while $\widehat{I}^P_{0z} > 0$. We note the time integral of $\widehat{I}^P_{0x} + \widehat{I}^P_{0y} + \widehat{I}^P_{0z}$ for the valid lapse time region is about 0.94 for the case of $V_0 t_M/z = 0.05$.

2.3. S Wave Envelopes

2.3.1. Parabolic Wave Equation

[31] Plane S waves having a polarization to the x direction propagating to the z direction are represented by a vector potential having only y component B_y, where $\mathbf{u} = (-\partial_z B_y, 0, \partial_x B_y)$. We note that three components of vector potential are independent each other as shown in (3). If we write $B_y = \phi$ and the S wave velocity as $\beta(\mathbf{x}) = V_0(1 + \xi(\mathbf{x}))$, the y component of vector potential ϕ satisfies wave equation (4). When the wavelengths are smaller than the correlation distance, if we write ϕ as a superposition of plane waves as (5), field U satisfies the parabolic wave equation (6).

2.3.2. Intensities

[32] For the incidence of S wavelet having a polarization to the x direction, the y component intensity is always zero,

$$I_y^S(\mathbf{x}_\perp, z, t) \equiv \left\langle \left| u_y(\mathbf{x}_\perp, z, t) \right|^2 \right\rangle = 0. \tag{42}$$

The z component intensity is given by

$$\begin{aligned} I_z^S(\mathbf{x}_\perp, z, t) &\equiv \left\langle |u_z(\mathbf{x}_\perp, z, t)|^2 \right\rangle \\ &= \left\langle \partial_{x'}\phi(\mathbf{x}'_\perp, z, t)\, \partial_{x''}\phi(\mathbf{x}''_\perp, z, t)^* \right\rangle_{\mathbf{x}'=\mathbf{x}''} \\ &= \frac{1}{2\pi}\int_{-\infty}^{\infty} d\omega' e^{ik'_0 z - i\omega' t} \\ &\quad \cdot \frac{1}{2\pi}\int_{-\infty}^{\infty} d\omega'' e^{-ik''_0 z + i\omega'' t} \left\langle \frac{\partial_{x'} U'}{k'_0} \frac{\partial_{x''} U''^*}{k''_0} \right\rangle_{\mathbf{x}'=\mathbf{x}''} \\ &= \frac{1}{2\pi}\int_{-\infty}^{\infty} d\omega_c \widehat{I}_z^S(z, t, \omega_c)\ , \end{aligned} \tag{43}$$

where the last line gives the definition of the intensity spectral density as

$$\begin{aligned} \widehat{I}_z^S(z, t, \omega_c) = \frac{1}{2\pi}\int_{-\infty}^{\infty} d\omega_d e^{-i\omega_d (t - z/V_0)} \\ \cdot \left[-\frac{\partial_{x_d}^2}{k_c^2}\, \Gamma_2(\mathbf{x}_{\perp d}, z, \omega_c, \omega_d) \right]_{\mathbf{x}_{\perp d}=0}. \end{aligned} \tag{44}$$

The x component intensity is given by

$$\begin{aligned} I_x^S(\mathbf{x}_\perp, z, t) &\equiv \left\langle |u_x(\mathbf{x}_\perp, z, t)|^2 \right\rangle \\ &= \left\langle \partial_z\phi(\mathbf{x}'_\perp, z, t)\, \partial_z\phi(\mathbf{x}''_\perp, z, t)^* \right\rangle_{\mathbf{x}'=\mathbf{x}''} \\ &= \frac{1}{2\pi}\int_{-\infty}^{\infty} d\omega' e^{ik'_0 z - i\omega' t} \frac{1}{2\pi}\int_{-\infty}^{\infty} d\omega'' e^{-ik''_0 z + i\omega'' t} \\ &\quad \cdot \left\langle \left(U' + \frac{\partial_z U'}{ik'_0} \right) \left(U''^* - \frac{\partial_z U''^*}{ik_0} \right) \right\rangle_{\mathbf{x}'=\mathbf{x}''} \\ &= \frac{1}{2\pi}\int_{-\infty}^{\infty} d\omega_c \widehat{I}_x^S(z, t, \omega_c), \end{aligned} \tag{45}$$

where the intensity spectral density is

$$\begin{aligned} \widehat{I}_x^S(z, t, \omega_c) &= \frac{1}{2\pi}\int_{-\infty}^{\infty} d\omega_d e^{-i\omega_d (t - z/V_0)} \\ &\quad \cdot \left[\left(1 + \frac{\Delta_{\perp d}}{k_c^2} \right) \Gamma_2(\mathbf{x}_{\perp d}, z, \omega_c, \omega_d) \right]_{\mathbf{x}_{\perp d}=0} \\ &= \widehat{I}^R(z, t, \omega_c) - 2\,\widehat{I}_z^S(z, t, \omega_c), \end{aligned} \tag{46}$$

where $\partial_{x_d}{}^2\, \Gamma_2 = \partial_{y_d}{}^2\, \Gamma_2$ is used because of the isotropy of randomness. We note that intensities are independent of transverse location $\mathbf{x}_\perp$ because of the homogeneity of randomness. The reference intensity spectral density I^R is given by (22) and (27), in which V_0 is the S wave velocity.

2.3.3. Gaussian Autocorrelation Function

[33] In the case of quasi monochormomatic waves, taking the same procedure as for P waves, we solve the master equation (12) for TFMCF. TFMCF Γ_2 is factorized into ${}_0\Gamma_2$ and the wandering term. For the case of random media characterized by a Gaussian ACF, we solve the master equation (30) for ${}_0\Gamma_2$ under the initial condition (25), which means the incidence of an impulsive plane S wavelet polarized to the x direction propagating to the z direction:

$$\widehat{I}_x^S(z, t, \omega_c) = \delta(t - z/V_0), \quad \widehat{I}_y^S(z, t, \omega_c) = \widehat{I}_z^S(z, t, \omega_c) = 0 \quad \text{for } z < 0. \tag{47}$$

The solution of (30) is given by (31) with (32) and (33), where V_0 is the average S wave velocity. By using this solution, we obtain the z component intensity spectral density without wandering effect as

$$\begin{aligned} \widehat{I}_{z0}^S(z, t, \omega_c) &= \frac{1}{2\pi}\int_{-\infty}^{\infty} d\omega_d e^{-i\omega_d (t - z/V_0)} \\ &\quad \cdot \left[-\frac{\partial_{x_d}^2}{k_c^2}{}_0\,\Gamma_2(\mathbf{x}_{\perp d}, z, \omega_c, \omega_d) \right]_{\mathbf{x}_{\perp d}=0} \\ &= \frac{V_0 t_M}{z} 2 \frac{\left(t - \frac{z}{V_0} \right)}{t_M} \widehat{I}_0^R(z, t, \omega_c) \\ &= \frac{V_0 t_M}{z} 2 \frac{\left(t - \frac{z}{V_0} \right)}{t_M} \frac{\pi}{8 t_M} \vartheta_1' \left(0, e^{-\frac{\pi^2 (t - z/V_0)}{4\ t_M}} \right) H\left(t - \frac{z}{V_0} \right). \end{aligned} \tag{48}$$

The x component intensity spectral density without wandering effect is given by

$$\begin{aligned} \widehat{I}_{x0}^S(z, t, \omega_c) &= \widehat{I}_0^R(z, t; \omega_c) - 2\,\widehat{I}_{z0}^S(z, t, \omega_c) \\ &= \left[1 - \frac{V_0 t_M}{z} \frac{4(t - z/V_0)}{t_M} \right] \widehat{I}_0^R(z, t, \omega_c) \\ &= \left[1 - \frac{V_0 t_M}{z} \frac{4(t - z/V_0)}{t_M} \right] \\ &\quad \cdot \frac{\pi}{8 t_M} \vartheta_1' \left(0, e^{-\frac{\pi^2 (t - z/V_0)}{4\ t_M}} \right) H\left(t - \frac{z}{V_0} \right). \end{aligned} \tag{49}$$

2.3.4. Characteristics of S Wave Envelopes

[34] For the case of $V_0 = 4.5$ km/s, $\varepsilon = 0.05$ and $a = 8$ km, Figure 5 (bottom) shows intensity spectral densities without wandering effect and those with wandering effect for the incidence of an impulsive plane S wavelet polarized to the x direction. We note that the y component is zero. Figure 6 (bottom) enlarges traces for the z component. Peak delay and envelope broadening are seen in both components; however, the peak delay of the z component is larger than that of the x component and the peak value of z component is smaller than that of x component at each travel distance. For the same fractional fluctuation for both P and S wave velocities, the envelope width of S wave is 1.73 times larger than that of P waves since the characteristic time is proportional to the reciprocal of the average wave velocity.

[35] For S waves, the time integral of the MS envelope of longitudinal component linearly increases with travel distance and the linear coefficient is the ratio of the MS fractional fluctuation to the correlation distance since

$$\int_{z/V_0}^{\infty} \widehat{I}_{z0}^S(z, t, \omega_c) dt = \frac{4 V_0 t_M}{z} = \frac{2\sqrt{\pi}\varepsilon^2}{a} z. \tag{50}$$

The time integral of transverse intensity spectral density without wandering effect is

$$\int_{z/V_0}^{\infty} \widehat{I}^S_{x0}(z,t,\omega_c)dt = 1 - \frac{8V_0 t_M}{z} = 1 - \frac{4\sqrt{\pi}\varepsilon^2}{a}z. \quad (51)$$

At large lapse times as $t > (5/4)(z/V_0)$, $\widehat{I}^S_{x0}$ becomes negative, which means the breakdown of the approximation.

3. Summary and Discussions

[36] Direct synthesis of vector wave envelopes in 3-D random elastic media is formulated on the basis of the Markov approximation in the case that wavelength is shorter than the correlation distance. Considering an ensemble of random elastic media, we have derived the stochastic master equation for the of potential field. The MS envelope of each vector component can be derived from the Fourier transform of TFMCF. For the incidence of an impulsive elastic plane wavelet to random elastic media characterized by a Gaussian ACF with a small fractional velocity fluctuation, vector wave envelopes are analytically written by using the elliptic theta function.

[37] For the incidence of an impulsive plane P wavelet, each of longitudinal and transverse component envelopes shows peak delay and envelope broadening with travel distance increasing. The transverse component has a smaller amplitude and a longer peak delay than the longitudinal component; however, the transverse component amplitude essentially reflects scattering and diffraction effects: the time integral of the MS amplitude of transverse component linearly increases with travel distance increasing, where the linear coefficient is the ratio of the MS fractional fluctuation of P wave velocity to the correlation distance. These theoretical results imply that the partition of energy to the transverse component could be a good stochastic measure of medium inhomogeneity of the crust and the most upper mantle in the teleseismic P wave envelope analysis. For the incidence of an impulsive plane S wavelet with a linear polarization, elastic waves have a polarization in the plane containing the initial polarization and the incident ray direction. Each of transverse and longitudinal component envelopes shows peak delay and envelope broadening with travel distance increasing. The envelope broadening of S waves is larger than that of P waves when the fractional fluctuation is the same for both P and S wave velocities. The longitudinal component has a smaller amplitude and a longer peak delay than the transverse component; however, the longitudinal amplitude reflects the scattering and diffraction effects: the time integral of the MS amplitude of longitudinal component linearly increases with travel distance increasing.

[38] It will be necessary to confirm this synthesis with numerical simulations for various values of fractional fluctuation and correlation distance to examine the validity range of this approximation as was done for the 2-D case. *Korn and Sato* [2005] confirmed the validity for the case of plane P and S wavelets of 2 Hz for travel distances 50 to 250 km in random elastic media characterized by a Gaussian ACF with $\varepsilon = 5\%$, $a = 5$ km and background velocities $\alpha_0 = 6$ km/s and $\beta_0 = 3.46$ km/s. In order to interpret vector seismogram envelopes of local earthquakes, it is necessary to develop the synthesis of vector wave envelopes for the spherical radiation from a point source in 3-D random elastic media. It is also interesting to extend the formulation to random elastic media having realistic power law spectrum since we can expect that envelope broadening is larger in higher frequencies in such a spectrum as predicted from scalar wave studies.

[39] **Acknowledgments.** The author is grateful to Anatoly Petukhin and Sergei Shapiro for their helpful comments. This work is partially supported by the Grant-in-Aid for Scientific Research 17540389 from JSPS and the sponsorship of JNES open application research project for enhancing the basis of nuclear safety.

References

Aki, K. (1973), Scattering of P waves under the Montana LASA, *J. Geophys. Res.*, *78*, 1334–1346.

Atkinson, G. M. (1993), Notes on ground motion parameters for eastern North America: Duration and H/V ratio, *Bull. Seismol. Soc. Am.*, *83*, 587–596.

Barabanenkov, Y. N., Yu. A. Kravtsov, S. M. Rytov, and V. I. Tatarskii (1971), Status of the theory of propagation of waves in randomly inhomogeneous medium, *Sov. Phys. Usp., Engl. Transl.*, *13*, 551–680.

Douglas, A., P. D. Marshall, P. G. Gibbs, J. B. Young, and C. Blamey (1973), P signal complexity re-examined, *Geophys. J. R. Astron. Soc.*, *33*, 195–221.

Fehler, M., H. Sato, and L.-J. Huang (2000), Envelope broadening of outgoing waves in 2-D random media: A comparison between the Markov approximation and numerical simulations, *Bull. Seismol. Soc. Am.*, *90*, 914–928.

Flatté, S. M., and R. S. Wu (1988), Small-scale structure in the lithosphere and asthenosphere deduced from arrival time and amplitude fluctuations at NORSAR, *J. Geophys. Res.*, *93*, 6601–6614.

Gusev, A. A., and I. R. Abubakirov (1996), Simulated wave envelopes of non-isotropically scattered body waves as compared to observed ones: Another manifestation of fractal heterogeneity, *Geophys. J. Int.*, *127*, 49–60.

Gusev, A. A., and I. R. Abubakirov (1999a), Vertical profile of effective turbidity reconstructed from broadening of incoherent body wave pulse-I. General approach and the inverse procedure, *Geophys. J. Int.*, *136*, 295–308.

Gusev, A. A., and I. R. Abubakirov (1999b), Vertical profile of effective turbidity reconstructed from broadening of incoherent body wave pulse-II. Application to Kamchatka data, *Geophys. J. Int.*, *136*, 309–323.

Hock, S., M. Korn, J. Ritter, and E. Rothert (2004), Mapping random lithospheric heterogeneities in northern and central Europe, *Geophys. J. Int.*, *157*, 251–264.

Ishimaru, A. (1978), *Wave Propagation and Scattering in Random Media*, vols. 1 and 2, Elsevier, New York.

Korn, M. (1993), Determination of site-dependent scattering Q from P wave coda analysis with an energy-flux model, *Geophys. J. Int.*, *113*, 54–72.

Korn, M. (1997), Modelling the teleseismic P coda envelope: Depth dependent scattering and deterministic structure, *Phys. Earth Planet. Inter.*, *104*, 23–36.

Korn, M., and H. Sato (2005), Synthesis of plane vector wave envelopes in 2-D random elastic media based on the Markov approximation and comparison with finite difference simulations, *Geophys. J. Int.*, *161*, 839–848.

Lee, L. C., and J. R. Jokipii (1975a), Strong scintillations in astrophysics. I. The Markov approximation, its validity and application to angular broadening, *Astrophys. J.*, *196*, 695–707.

Lee, L. C., and J. R. Jokipii (1975b), Strong scintillations in astrophysics. II. A theory of temporal broadening of pulses, *Astrophys. J.*, *201*, 532–543.

McLaughlin, K. L., and L. M. Anderson (1987), Stochastic dispersion of short-period P waves due to scattering and multipathing, *Geophys. J. R. Astron. Soc.*, *89*, 933–963.

Nishimura, T., K. Yoshimoto, T. Ohtaki, K. Kanjo, and I. Purwana (2002), Spatial distribution of lateral heterogeneity in the upper mantle around the western Pacific region as inferred from analysis of transverse components of teleseismic P coda, *Geophys. Res. Lett.*, *29*(23), 2137, doi:10.1029/2002GL015606.

Obara, K., and H. Sato (1995), Regional differences of random inhomogeneities around the volcanic front in the Kanto-Tokai area, Japan, revealed form the broadening of S wave seismogram envelopes, *J. Geophys. Res.*, *100*, 2103–2121.

Petukhin, A. G., and A. A. Gusev (2002), The duration-distance relationship and average envelope shapes of small Kamchatka earthquakes, *Pure Appl. Geophys.*, *160*, 1717–1743.

Ritter, J. R. R., P. M. Mai, G. Stoll, and K. Fuchs (1997), Scattering of teleseismic waves in the lower crust observations in the Massif Central, France, *Phys. Earth Planet. Inter.*, *104*, 127–146.

Saito, T., H. Sato, and M. Ohtake (2002), Envelope broadening of spherically outgoing waves in three-dimensional random media having power law spectra, *J. Geophys. Res.*, *107*(B5), 2089, doi:10.1029/2001JB000264.

Sato, H. (1989), Broadening of seismogram envelopes in the randomly inhomogeneous lithosphere based on the parabolic approximation: Southeastern Honshu, Japan, *J. Geophys. Res.*, *94*, 17,735–17,747.

Sato, H., and M. Fehler (1998), *Seismic Wave Propagation and Scattering in the Heterogeneous Earth*, 308 pp., Springer, New York.

Scherbaum, F., and H. Sato (1991), Inversion of full seismogram envelopes based on the parabolic approximation: Estimation of randomness and attenuation in southeast Honshu, *Japan, J. Geophys. Res.*, *96*, 2223–2232.

Shishov, V. L. (1974), Effect of refraction on scintillation characteristics and average pulsars, *Sov. Astron.*, *17*, 598–602.

Sreenivasiah, I., A. Ishimaru, and S. T. Hong (1976), Two-frequency mutual coherence function and pulse propagation in a random medium: An analytic solution to the plane wave case, *Radio Sci.*, *11*, 775–778.

Tatarskii, V. I. (1971), *The Effects of the Turbulent Atmosphere on Wave Propagation*, Israel Program for Sci. Transl., Jerusalem.

Wagner, G. S. (1997), Regional wave propagation in southern California and Nevada: Observations from a three-component seismic array, *J. Geophys. Res.*, *102*, 8285–8311.

Williamson, I. P. (1972), Pulse broadening due to multiple scattering in the interstellar medium, *Mon. Not. R. Astron. Soc.*, *157*, 55–71.

Wolfram, S. (1999), *Mathematica*, version 4, 1470 pp., Cambridge Univ. Press, New York.

H. Sato, Geophysics, Science, Tohoku University, Aramaki-Aza-Aoba 6-3, Aoba-ku, Sendai-shi, Miyagi-ken 980-8578 Japan. (sato@zisin.geophys.tohoku.ac.jp)